Single-Ended and Fully-Differential Current-Input Current-Output Universal Frequency Filter with Transconductace and Transresistance Amplifiers

L. LANGHAMMER, J. JERABEK J. POLAK and P. CIKA
Department of Telecommunications, Faculty of Electrical Engineering and Communication
Brno University of Technology
Technicka 12, 616 00, Brno
CZECH REPUBLIC
langhammer@phd.feec.vutbr.cz, jerabekj@feec.vutbr.cz, xpolak24@phd.feec.vutbr.cz, cika@feec.vutbr.cz

Abstract: - A new filtering structure of the 2nd-order universal frequency filter is presented. The proposed filter operates in a current-input current-output form and it is designed using signal-flow graphs (SFG) method. Operational transconductance amplifiers (OTAs), current follower (CF) and operational transresistance amplifier (OTRA) are used in the proposal. The filter possesses ability to adjust the pole frequency and quality factor of the filter without violating each other. All output responses are taken directly from high-impedance outputs of used active elements. The proposal requires only two external passive elements, namely two capacitors which are both grounded. The proposed filter has been also designed in its fully-differential form. The proper function of the proposed S-E and F-D filter is verified by PSpice simulations and in case of the S-E filter also by experimental measurements. Demonstrations of possibility to tune the pole frequency and quality factor of the proposed S-E and F-D filter are illustrated in the paper. Subsequently, comparison of simulations of S-E and F-D structures of the proposed filter and comparison of results of the S-E filter obtained from simulations and experimental measurements are also included.

Key-Words: -Frequency filter, Transconductance amplifier, Transresistance amplifier, Simulation, Experimental measurement.

1 Introduction

Analogue frequency filters have a wide variety of use in electrical circuits such as telecommunication, measurement technology, radio-technology, electro-acoustics etc. Recently, we have experienced tendency of reducing the size of integrated circuits in order to decrease energy consumptions. Such a process also leads to decrease in supply voltage of circuits and decrease in the level of processed signals. This subsequently results in reduction of signal-to-noise ratio and limiting of the dynamic range of the circuit. Therefore, the design of electrical circuits currently focuses on active elements operating in a current-mode due to the advantages which can be achieved in particular cases. Among the advantages there are better signal-to-noise ratio, wider frequency bandwidth, greater dynamic range and lower power consumption [1].

To mention some types of current active elements, we can encounter frequency filters using different types of current conveyors (CC) such as current conveyors of the second generation (CCII) [2], current controlled conveyors (CCC) [3-5], inverting current conveyors (ICCII) [6] and differential voltage current conveyors (DVCC) [7]. Furthermore, it is possible to come across a variety of transconductance amplifiers, for example frequency filters with operational transconductance amplifiers (OTA) [8-10], current differencing transconductance amplifiers (CDTA) [11, 12], current follower transconductance amplifiers (CFTA) [13, 14], current controlled current conveyor transconductance amplifier (CCCCTA) [15, 16], current following cascaded transconductance amplifier (CFCTA) [17] and Z-copy current inverter transconductance amplifiers (ZC-CITA) [18, 19]. Frequency filters employing current followers (CF) can be found for instance in [8, 10, 20-24]. Frequency filters with digitally controlled current followers (DCCF) are described for example in [25, 26]. We can also mention filters using digitally adjustable current amplifier (DACA) [20-23].

Table 1: Comparison of previously reported filters

Reference	Year	Number of active elements	Number of passive elements	Independent tuning of f_0	Independent tuning of Q	Experimental measurement	Type of used active element(s)	All responses taken from high-impedance outputs	All capacitors grounded	Transfer functions
[2]	2009	3	5	Yes	Yes	No	DO-CCII	Yes	Yes	All
[3]	2009	3	2	Yes	Partly	No	MO-CCCIIs	Yes	Yes	All
[4]	2008	1	3	Yes	Partly	No	CCCII	No	Yes	All
[5]	2004	2	2	Yes	Partly	No	CCCII	No	No	All
[6]	2012	3	5	Yes	Yes	No	DO-ICCII	Yes	Yes	All
[7]	2012	3	5	Yes	Yes	No	DVCC	Yes	Yes	All
[8]	2011	3	2	Yes	Partly	Yes	CF, OTA	Yes	Yes	All
[9]	2009	3	3	Yes	Yes	Yes	OTA	Yes	Yes	All
[10]	2010	4	2	Yes	Partly	No	CF, OTA	Yes	Yes	All
[11]	2008	1	3	Yes	Partly	No	CDTA	No	Yes	All
[12]	2005	3	2	Yes	Partly	No	CDTA	Yes	Yes	All
[13]	2014	3	2	Yes	Yes	No	CFTA	Yes	Yes	All
[14]	2014	2	2	Yes	Partly	No	ZC-CFTA	Yes	Yes	All
[15]	2012	2	2	Yes	Yes	No	CCCCTA	Yes	Yes	All
[16]	2009	3	2	Yes	Partly	No	CCCCTA	Yes	No	All
[17]	2014	1	2	Yes	Partly	No	CFCTA	Yes	Yes	All
[18]	2009	2	2	Yes	Partly	Yes	ZC-CITA	Yes	Yes	All
[19]	2010	2	2	Yes	Partly	No	ZC-CITA	Yes	Yes	All
[20]	2013	5/6	4/4	Yes	Yes	No	CF, DACA	Yes	Yes	All
[21]	2012	4	4	Yes	Yes	No	CF, DACA	Yes	Yes	All
[22]	2013	3/4	4/4	Yes	Yes	No	CF, DACA	Yes	Yes	BP
[23]	2009	6	6	Yes	No	No	CF, DACA	Yes	Yes	LP, BP
[24]	2006	2	2	Yes	Partly	No	DO-CF	Yes	Yes	All
[25]	2008	6	5	Yes	Yes	Yes	DCCF	Yes	Yes	All
[26]	2009	6	4	Yes	Yes	No	DCCF	Yes	Yes	All
proposal	-	*5*	*2*	*Yes*	*Yes*	*Yes*	*CF, OTA, OTRA*	*Yes*	*Yes*	*All*

DO-CCII – Dual-Output Second Generation Current Conveyor
DO-(MO)-CCCII– Dual-Output (Multi-Output) Second Generation Current Controlled Conveyor
DO-ICCII – Dual-Output Inverting Second generation Current Conveyor
DVCC – Differential Voltage Current Conveyor
(DO)-CF – (Dual-Output) Current Follower
OTA – Operational Transconductance Amplifier
CDTA – Current Differencing Transconductance Amplifier
CFTA – Current Follower Transconductance Amplifier
ZC-CFTA – Z-copy Current Follower Transconductance Amplifier
CCCCTA – Current Controlled Current Conveyor Transconductance Amplifier
CFCTA – Current Following Cascaded Transconductance Amplifier
ZC-CITA – Z-copy Current Inverter Transconductance Amplifier
DACA – Digitally Adjustable Current Amplifier
DCCF – Digitally controlled current follower
OTRA – Operational Transresistance Amplifier

Fully-differential (F-D) structures have some advantages in comparison to the single-ended (S-E) circuits such as lower harmonic distortion, possibility of greater dynamic range of the processed signals, greater attenuation of common-mode signals and better power supply rejection ratio. F-D structures have also a few drawbacks that their design is more complex than in case of single-ended structures which leads to a larger area taken on the chip and higher power consumption [19].

A comparison of the previously reported [2-26] filtering structures is given in Tab.1. As it can be seen the proposed structures suffer from one or more drawbacks:

- The structures contain at least one floating capacitor which is not suitable for the implementation and integrability of the circuit [5, 16].
- Not all currents responses are taken from the high-impedance outputs [5, 11].
- Filters require external resistors causing an increase of the power consumption and area taken on the chip [2, 6, 7, 9, 20-23, 25, 26].
- The quality factor and characteristic frequency cannot be both set fully continuously without affecting one another [3-5, 8, 10-12, 14, 16-19 23, 24].
- Filters consist of more inputs (require copies of the input currents to obtain particular transfer functions) [3, 6, 7, 12, 24].
- Additionally, only the structures in [8, 9, 18, 25] are supported by the experimental measurements of the proposed filters.

For the analysis and synthesis of linear electrical networks, Mason-Coates' (M-C) graphs [27] can be used. These graphs can be understood as diagrams of nodes which represent variables and directed branches which define mutual relationships between nods of the analyzed structure.

Transfer function of the graph is determined by Manson's gain formula:

$$K = \frac{1}{\Delta}\sum_i P_i \Delta_i , \tag{1}$$

where P_i represents gain of i-th forward path and Δ is the determinant of the graph which is given by:

$$\Delta = P - \sum_i P_i \Delta_i + \sum_j P_j \Delta_j - \sum_k P_k \Delta_k + \ldots , \tag{2}$$

where P represents self-loop products, P_i stands for individual loop gains, P_j is products of two non-touching loops, P_k represents products of three non-touching loops, Δ_i, Δ_j and Δ_k are loop gain terms which do not touch the i-th, j-th and k-th forward paths etc.

2 Description of used active elements

The proposed filters consist of three types of active elements which are described in this section. The schematic symbols, M-C graphs and eventual realization of used active elements are also included.

The first used active element is an operational transconductance amplifier (OTA), balanced operational transconductance amplifier (BOTA) [8] and multi-output operational transconductance amplifier (MOTA) [9], respectively. The schematic symbol and M-C graph of the BOTA element can be seen in Fig. 1 a), b). It consists of two balanced

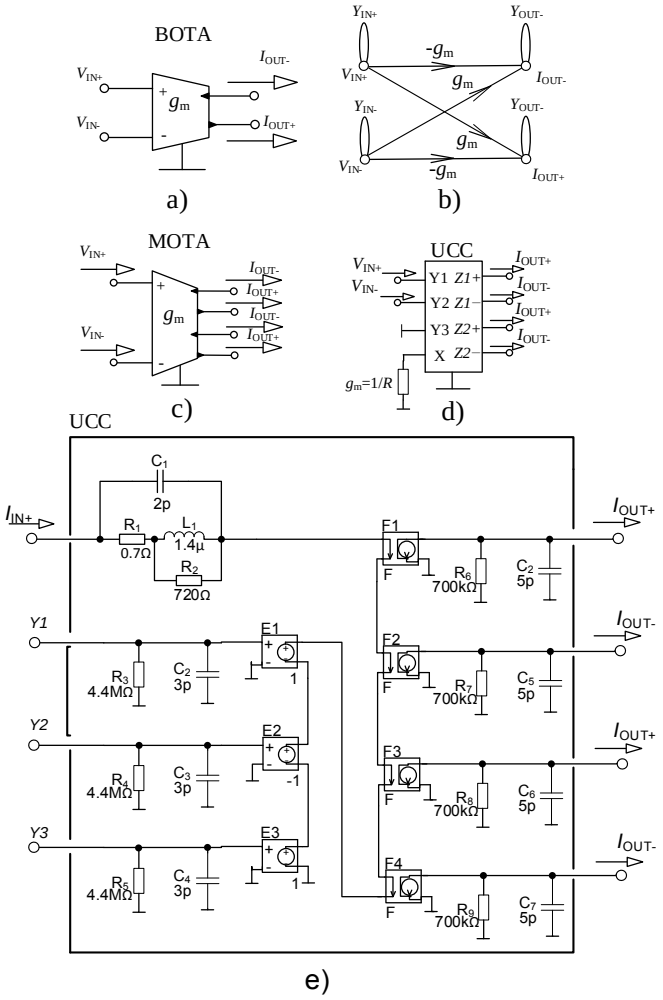

Fig. 1. a) Schematic symbol of the BOTA, b) M-C graph of the BOTA, c) schematic symbol of the MOTA, d) possible implementation of the MOTA using the UCC-N1B device, e) used simulation model of the UCC

inputs and outputs. For our purposes, more output terminals of this active element are required. By adding two more output terminals we obtain a multiple-output transconductance amplifier (MOTA). The schematic symbol of this element and its possible implementation using a universal current conveyor (UCC) [28] are illustrated in Fig. 1 c), d). The model of the UCC used for simulations is presented in Fig 1 e). This simulation model is common for all active elements since the UCC can be used to build all used active elements. Transconductance g_m of this alternative solution can be set by resistor R according to relation $g_m = 1/R$.

The BOTA element is described by following relation:

$$I_{OUT+} = -I_{OUT-} = g_m(V_{IN+} - V_{IN-}), \quad (3)$$

where g_m is the transconductance of this active element.

The next used active element is a multi-output current follower (MO-CF) [29]. Its schematic symbol, M-C graph and possible implementation using the UCC-N1B device is presented in Fig. 2 a), b), c) respectively.

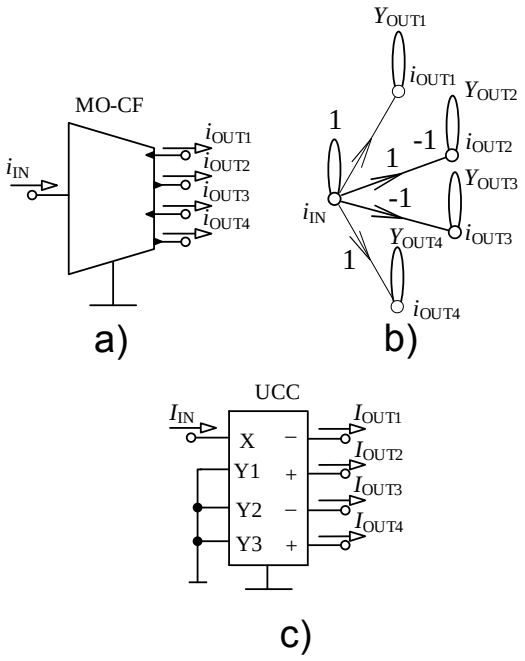

Fig. 2. Multi-output current follower a) schematic symbol, b) M-C graph, c) possible implementation using the UCC-N1B device

The MO-CF possesses one input and four output terminals. The relations between input and output currents are as follows:

$$I_{OUT1} = I_{OUT3} = -I_{IN}, \quad (4)$$

$$I_{OUT2} = I_{OUT4} = I_{IN}. \quad (5)$$

In case of the fully-differential filter, a fully-differential current follower (FD-CF) is used. Such an element can be practically implemented by using a digitally adjustable current amplifier (DACA) [23], which possesses differential inputs and outputs.

The last used active element is an operational transresistance amplifier (OTRA) [30]. Figure 3 a), b) shows the schematic symbol and M-C graph of this element in a fully-differential form. A simple non-differential OTRA can be implemented by one UCC, or for example by two current feedback operational amplifiers (CFOA) [31]. Figure 3 c) illustrates possible implementation of this element in its F-D form using two universal current conveyors.

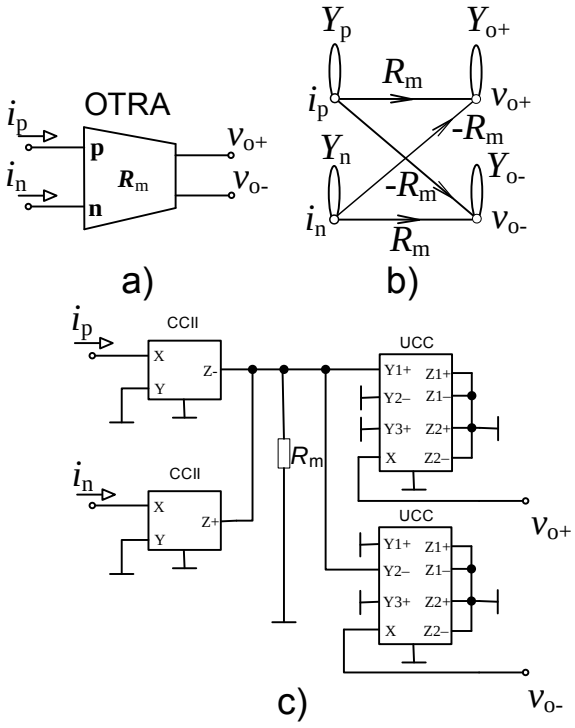

Fig. 3. Fully-differential operational transresistance amplifier a) schematic symbol, b) M-C graph c) possible implementation using two UCC-N1B devices

This active element in its F-D form consists of two current input terminals and two voltage output terminals. Resistance R_m implemented by a resistor connected between these components allow us to adjust transresistance of the OTRA element.

The OTRA can be described by equations:

$$v_{o+} = R_m(i_p - i_n), \quad (6)$$

$$v_{o-} = -R_m(i_p - i_n). \quad (7)$$

3 Filter proposal

The proposal focused on designing a 2nd-order universal current-input current-output frequency filter. Furthermore, the filter possesses possibility to adjust the pole frequency and quality factor of the filter without violating each other. The filter has been proposed using signal-flow graphs (SFGs) method. The circuit structure and its simplified M-C graph (selected for its simplicity and practical utilization) are illustrated in Fig. 4 a), b). It consists of one MO-CF, one BOTA, two MOTAs and one OTRA elements. The MOTA2 element has been added to the circuit structure because the voltage output of the OTRA cannot be directly connected to the current input of the filter. This might seem rather complicated and it is possible to choose other simpler solutions, for example using one current-input current-output active element etc. Nevertheless, used active elements (OTRA, OTA) are still relatively simple circuits, therefore, their use is not so critical to complexity of the whole circuit. Further simplification of the proposed filter can be eventually made. The fully-differential structure of the proposed filter can be seen in Fig. 5. The F-D filter consists of three MOTAs, one fully-differential version of the OTRA element and the MO-CF element has been replaced with a FD-CF.
The denominator of all transfer functions which is common for both filters is given by:

$$D = s^2 C_1 C_2 + s C_2 g_{m1} g_{m3} R_m + g_{m1} g_{m2}. \tag{8}$$

The pole frequency of the S-E and F-D filter can be tuned by changing values of $g_{m1}g_{m2}$ when $g_{m1} = g_{m2}$ and the quality factor remains the same. The quality factor is adjusted by changing g_{m3} and/or R_m without disturbing pole frequncy to any desired value. Another possible way (not used in our case) is to change the quality factor by changing transconductances g_{m1} and g_{m2}. Nevertheless, it would be necessary to change these values according to the condition $g_{m1}.n = g_{m2}/n$ (where n is unsigned integer) in order to avoid affecting the pole frequency which prevents us to change the value of the quality factor continuously. In this case, it would be possible only with discrete steps.

The pole frequency and quality factor of the S-E and F-D filter are defined accordingly:

$$f_0 = \frac{1}{2\pi}\sqrt{\frac{g_{m1}g_{m2}}{C_1 C_2}}, \tag{9}$$

$$Q = \frac{1}{g_{m3}R_m}\sqrt{\frac{g_{m2}C_1}{g_{m1}C_2}}, \tag{10}$$

where f_0 is the pole frequency of the filter, Q is the filter quality factor, g_{m1}, g_{m2}, g_{m3} are transconductances of OTA elements and R_m is the transresistance of the OTRA. As it can be seen from relations (9) and (10), the pole frequency can be set without violating the quality factor by changing values of transconductances g_{m1} and g_{m2} when $g_{m1} = g_{m2}$and the quality factor can be adjusted without violation of the pole frequency by changing g_{m3} and/or R_m.

The transfer functions of both proposed filters are described by equations:

$$\frac{I_{LP+}}{I_{IN}} = \frac{g_{m1}g_{m2}}{D}, \tag{11}$$

$$\frac{I_{BP-}}{I_{IN}} = \frac{-sC_2 g_{m1} g_{m3} R_m}{D}, \tag{12}$$

$$\frac{I_{HP+}}{I_{IN}} = \frac{s^2 C_1 C_2}{D}, \tag{13}$$

$$\frac{I_{BS+}}{I_{IN}} = \frac{I_{LP+} + I_{HP+}}{I_{IN}} = \frac{s^2 C_1 C_2 + g_{m1}g_{m2}}{D}, \tag{14}$$

$$\frac{I_{AP+}}{I_{IN}} = \frac{I_{LP+} + I_{BP-} + I_{HP+}}{I_{IN}} = \frac{s^2 C_1 C_2 - sC_2 g_{m1} g_{m3} R_m + g_{m1}g_{m2}}{D}. \tag{15}$$

From equations (11-15) is obvious that the proposed filters are universal, which means it is possible to obtain all standard transfer functions, namely low-pass, band-pass, high-pass, band-stop and all pass transfer functions. Furthermore, all transfer functions correspond with particular term of the denominator, therefore they have the unity gain in pass-band area regardless the values of g_m and R_m parameters (no matching is required for unity gain). All transfer functions are taken directly from high-impedance outputs of the active elements.

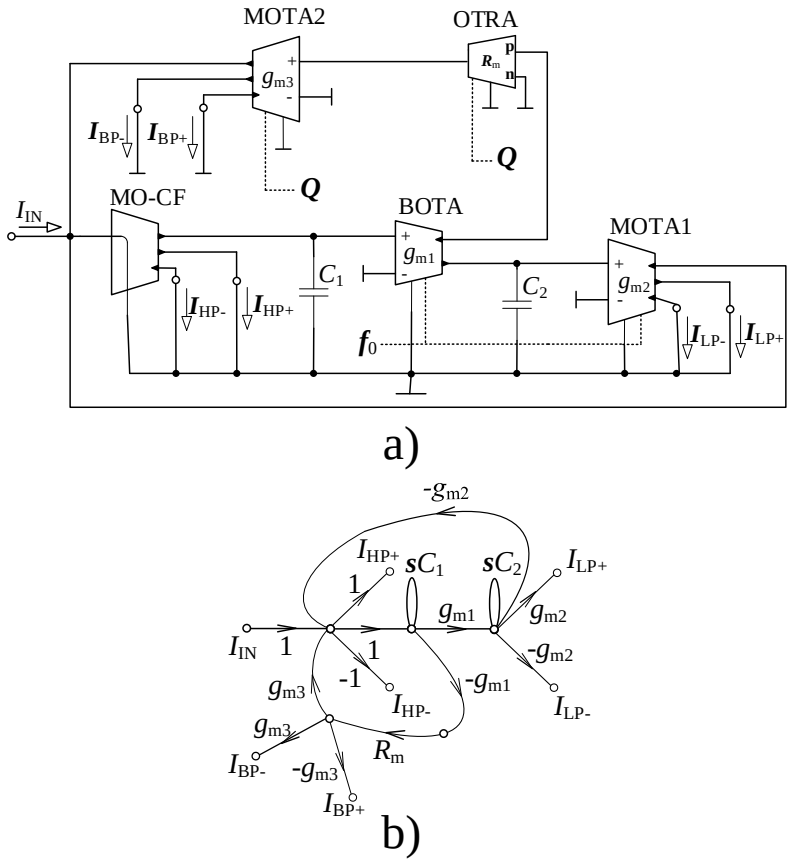

Fig. 4. Proposed S-E filter: a) circuit structure, b) simplified M-C graph

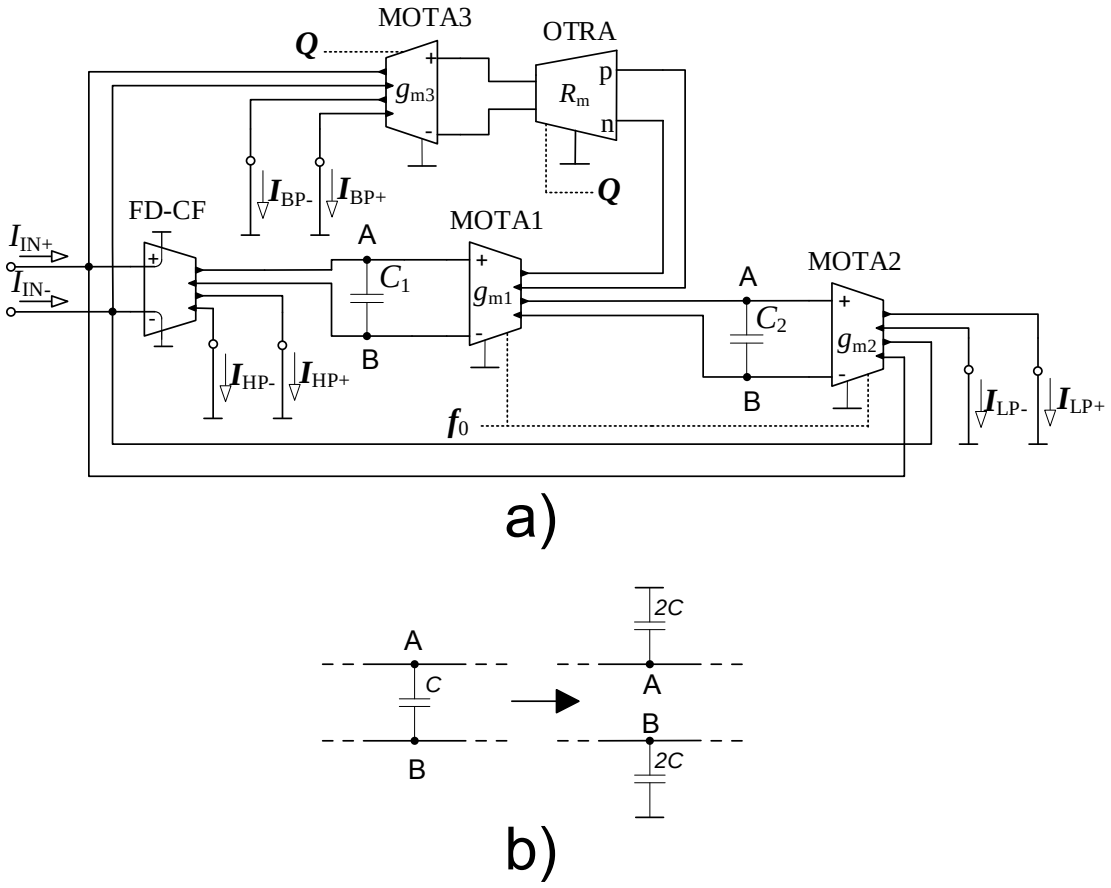

Fig. 5. Proposed F-D filter: a) circuit structure, b) implementation of non-floating conductances between nodes A and B

4 Simulation and experimental results

The simulation and also experimental results were carried out to verify appropriate function of the proposed filters. Simulations are performed using PSpice. The experimental results were performed by measurements of the implemented S-E filter in form of the printed circuit board (PCB), using a network analyzer Agilent 4395A and V/I, I/V converters. Converters are implemented using integrated circuits OPA860 [32] and OPA861 [33]. All output responses included in this paper are non-inverting transfer functions. All active elements used for simulations/experimental measurements were implemented using the UCC as suggested in section 2.

Values of the specific filter parameters for the PSpice simulations and experimental measurements have been stated accordingly: the starting pole frequency f_0 = 500 kHz, the starting quality factor Q = 0.707 (Butterworth approximation), values of capacitors C_1 = 470 pF and C_2 = 47 pF. The values of the capacitances were set accordingly in order to acquire the same value of transconductance g_{m1} g_{m2}, so the transconductances can be set simultaneously without affecting the quality factor of the proposed filter. Since we are changing values of the transconductances instead of changing values of the capacitances to adjust the pole frequency of the filter, it is easier to keep values of the transconductances of the same value than the opposite case. Of course it is possible to have the capacitances of the same value and the transconductances with ratio 1:10, or some other suitable ratio of both capacitances and transconductances. Values of transconductances g_{m1}, g_{m2} are calculated according to following relation:

$$g_{m1,2} = 2\pi f_0 \sqrt{C_1 C_2} = 0.467 \quad mS. \tag{16}$$

Thus, resistors of values of 2 kΩ which corresponds with transconductances of values of 0.5 mS have been chosen. The pole frequency is then equal to 535.42 kHz. The starting transresistance R_m is equal to 510 Ω, the starting value of g_{m3} has been then calculated from (17) in order to obtain the quality factor of value of 0.707.

$$g_{m3} = \frac{1}{QR_m}\sqrt{\frac{g_{m2}C_1}{g_{m1}C_2}} = 8.770 \quad mS, \tag{17}$$

which is approximately 114 Ω, therefore resistor of a value of 110 Ω has been used. Recalculated quality factor for these values is 0.682.

All values are the same for both S-E and F-D structure except the F-D value of transresistance R_m which must be 1/4 of the value used for the S-E filter to obtain the same value of the quality factor.

Figures 6-9 compare the simulation results of the S-E and F-D structure of the proposed filter. A comparison of simulation and experimental results of the S-E filter can be found in Figs. 10-13.

A comparison of the simulations of low-pass, band-pass, high-pass and band-stop transfer functions of the proposed S-E and F-D filter can be seen in Fig. 6. The obtained slope of attenuation of high-pass transfer functions (blue lines) is 38 dB per decade, 19 dB per decade for band-pass functions (red lines) and in case of low-pass transfer functions it is 40 dB per decade when the theoretical slopes are 40 dB per decade in case of high and low-pass transfer functions and 20 dB per decade for band-pass transfer function. The biggest attenuation of the band-stop function is 28 in case of the S-E filter and 24 for the F-D filter. The transfer functions are relatively similar to each other except the high-pass transfer function where we can see that the transfer functions significantly differ at lower frequencies.

The simulation results of adjustability of the pole frequency of the S-E and F-D filter are illustrated in Fig. 7.For this purpose, low-pass transfer function has been chosen as an example. Values of transconductances $g_{m1}g_{m2}$ have been set to (0.256 mS, 0.5 mS and 1 mS).Calculated values of the pole frequencies for chosen values are {274.57 kHz, 535.42 kHz, 1070.83 kHz}.Values of the pole frequencies obtained from the S-E filter are {232.16 kHz, 464.15 kHz, 1140.23 kHz} and values obtained from the F-D filter are {272.90 kHz, 575.40 kHz, 1905.46 kHz}. It can be seen that the S-E filter is closer to calculated values.

Figure 8 demonstrates the simulation results of the S-E and F-D filter when verifying a possibility of adjusting the quality factor of the proposed filter. In this case, band-pass transfer function has been used and parameter g_{m3} is changing when transresistance R_m is fixedly set to value of 510 Ω (127.5 Ω in case of the F-D structure).Values of g_{m3} are set accordingly: g_{m3} = (9.09 mS, 4.55 mS and 2.33 mS).Calculated values of the quality factors for these values of $g_{m3}$are {0.68, 1.36, 2.67}. Values of quality factors obtained in case of the S-E filter are {0.50, 1.37, 3.22} and {0.56, 1.55, 3.92} for the F-D structure. From the graph it can be seen that the pole frequency of individual functions is slightly changing to lower frequencies when the quality factor increases.

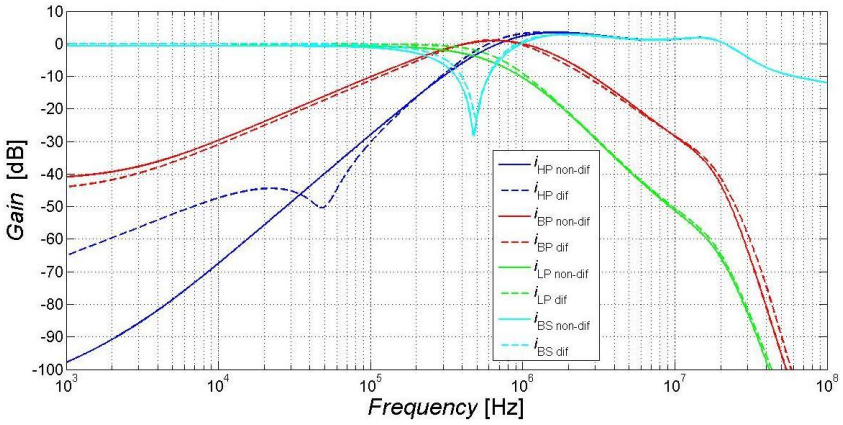

Fig. 6. Comparison of simulated transfer functions high-pass, band-pass, low-pass, band-stop of the proposed filter: S-E structure from Fig. 4 (solid lines) and F-D structure from Fig. 5 (dashed lines)

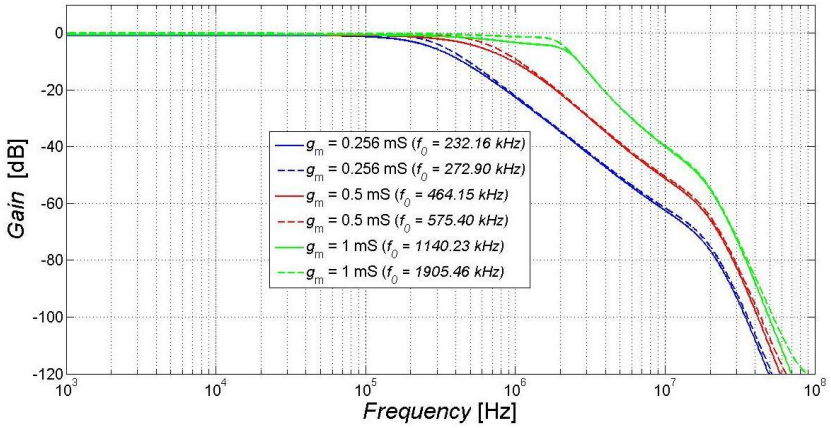

Fig. 7. Demonstration of possibility of adjusting the pole frequency of the proposed filter in case of the LP function: S-E structure from Fig. 4 (solid lines) and F-D structure from Fig. 5 (dashed lines)

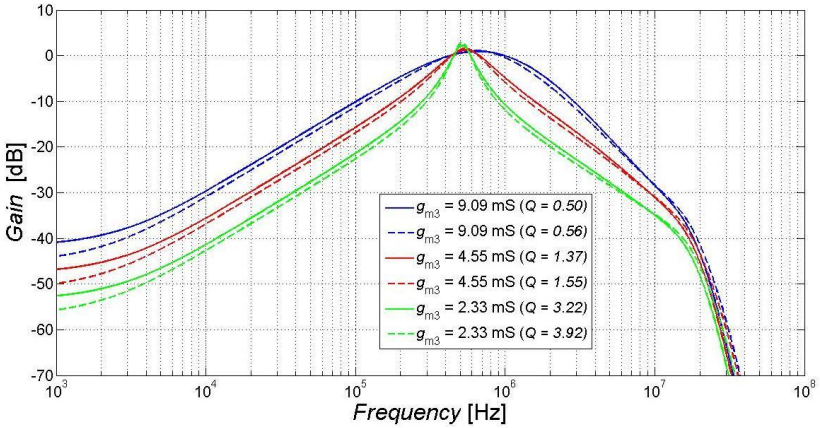

Fig. 8. Demonstration of possibility of adjusting the quality factor of the proposed filter when changing g_{m3}: S-E structure from Fig. 4 (solid lines) and F-D structurefrom Fig. 5 (dashed lines)

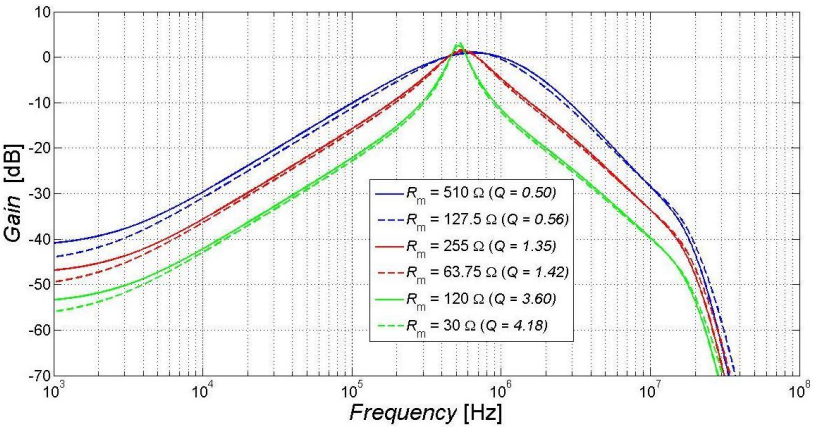

Fig. 9. Demonstration of possibility of adjusting the quality factor of the proposed filter when changing R_m: S-E structurefrom Fig. 4 (solid lines) and F-D structurefrom Fig. 5 (dashed lines)

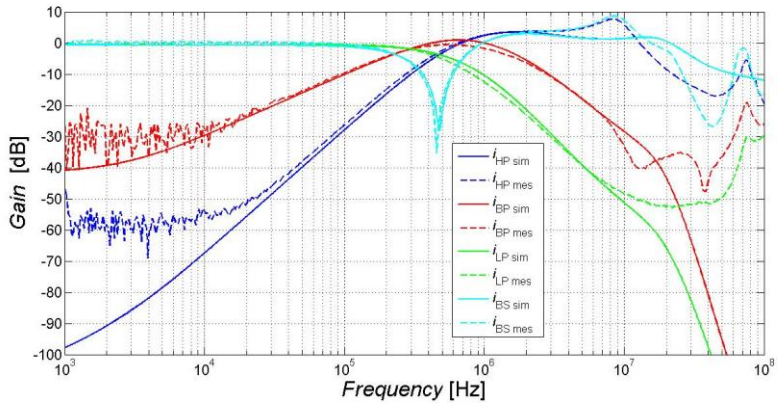

Fig. 10. Comparison of transfer functions high-pass, band-pass, low-pass, band-stop of the proposed S-E filter from Fig. 4: simulation (solid lines) and measured (dashed lines) results

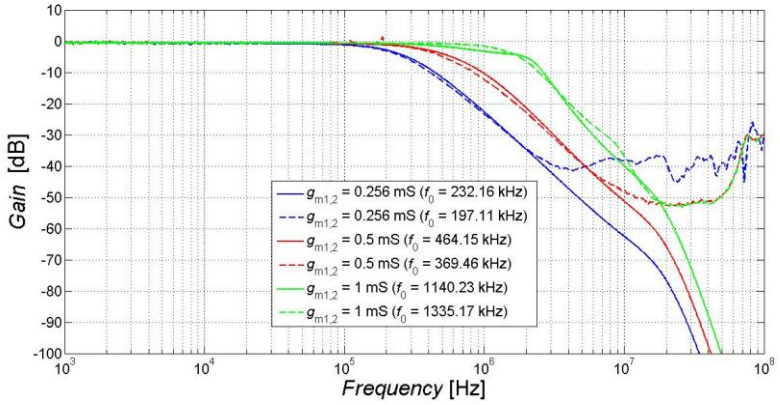

Fig. 11. Demonstration of possibility of adjusting the pole frequency of the proposed S-E filter from Fig. 4 in case of the LP function: simulation (solid lines) and experimental (dashed lines) results

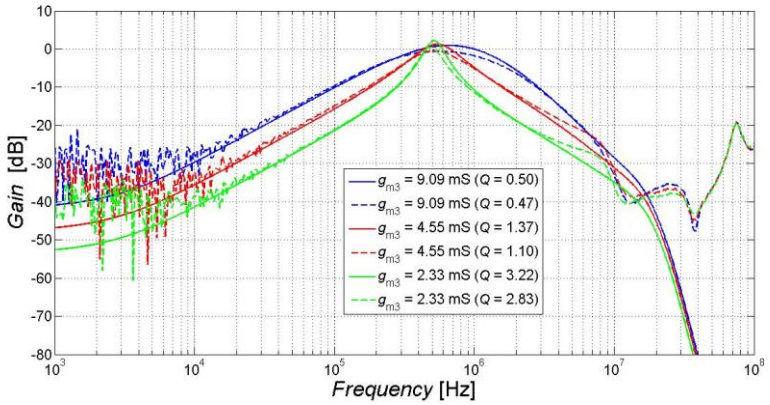

Fig. 12. Demonstration of possibility of adjusting the quality factor of the proposed S-E filter from Fig. 4 when changing g_{m3}: simulation (solid lines) and experimental (dashed lines) results

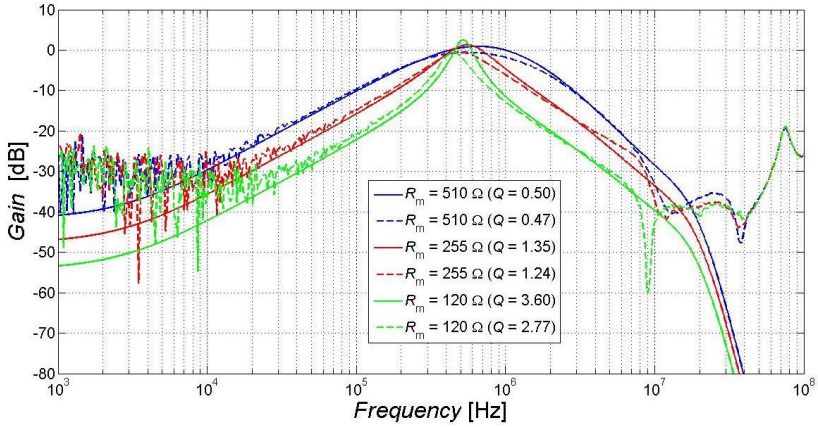

Fig. 13. Demonstration of possibility of adjusting the quality factor of the proposed S-E filter from Fig. 4 when changing R_m: simulation (solid lines) and experimental (dashed lines) results

A comparison of simulations of a possibility to adjust the quality factor when changing the transresistance R_m is shown in Fig. 9. Chosen values of the transresistance R_m are (510 Ω, 255 Ω, 120 Ω) which corresponds with values (127.5 Ω, 63.75 Ω, 30 Ω) used in case of the F-D structure, when g_{m3} = 9.09 mS. Calculated values of the quality factor of the S-E and F-D filter for these values are {0.68 , 1.36, 2.67}. Quality factors obtained from the S-E structure are {0.50, 1.35, 3.60} and values obtained from the F-D structure are {0.56, 1.42, 4.18}.From the graph it can be again seen that the pole frequency of individual functions is slightly decreasing when the quality factor is increasing.

Figure 10 shows simulated and measured low-pass, band-pass, high-pass and band-stop transfer functions of the proposed filter. The slope of attenuation of independent transfer functions is almost the same for both simulation and measurement of the S-E filter. High-pass transfer functions (blue lines) have the slope of attenuation of 38 dB per decade, band-pass functions (red lines) have 19 dB per decade and in case of low-pass transfer functions it is 40 dB per decade. The biggest attenuation of the band-stop function is 27 in case of the simulated results and 35 for the measured results. It can be seen that the filter can be suitably used approximately up to frequency of 6 MHz because of bandwidth limitations of used active elements. The measured results are affected mostly by output impedances (they are not high enough) of the active elements in the structure. The output impedance of the BOTA is the most dominant parasitic element mainly at lower frequencies because it is connected to node with C_2.Internal node of the OTRA with R_m connected also significantly affects measured results at higher frequencies because output impedance of the first stage (CCII) is not high enough with respect to R_m values. The results are also affected by limitations of used V/I, I/V converters.

A possibility of adjusting the pole frequency of the proposed filter is shown in Fig. 11. Values of parameters g_{m1} g_{m2} have been set accordingly: g_{m1} = g_{m2} = (0.256 mS, 0.5 mS and 1 mS). Calculated values of the pole frequency for these chosen values are {274.57 kHz, 535.42 kHz, 1070.83 kHz}. Values of the pole frequencies obtained from simulations are {232.16 kHz, 464.15 kHz, 1140.23 kHz} and values obtained by experimental measurements are {197.11 kHz, 369.46 kHz, 1335.17 kHz}.

Tuning the quality factor of the filter by changing g_{m3} is illustrated in Fig. 12. Values of g_{m3} are as follows: g_{m3} = (9.09 mS, 4.55 mS and 2.33 mS) when R_m is 510 Ω. Calculated values of the quality factor of the filter for these values are {0.68 , 1.36, 2.67}. Values of obtained quality factors are {0.50, 1.37, 3.22} in case of simulations and {0.47, 1.10, 2.83} for experimental measurement.

A possibility of adjusting the quality factor of the filter by changing transresistance R_m is shown in Fig. 13. Also in this case, band-pass transfer function has been used for the demonstration. Values of R_m have been selected accordingly: (510 Ω, 255 Ω, 120 Ω) when g_{m3} = 9.09 mS. Calculated values of the quality factor for these values are {0.68, 1.36, 2.90}. Quality factors obtained from simulations are {0.50, 1.35, 3.60} when values obtained during the experimental measurement are {0.47, 1.24, 2.77}.

5 Conclusion

The proper function and correctness of the proposed S-E and F-D filter has been verified by carrying out simulations and in case of the S-E filter also by the experimental measurements. Some simulation and experimental results are illustrated in the paper. From relations (11 - 15) it can be seen that the S-E and F-D proposed filter is universal because we can obtain all transfer functions. Furthermore, all transfer functions match the particular term of the denominator, therefore they have the unity gain in pass-band area regardless the values of g_m and R_m parameters. Comparing the slope of attenuation of individual transfer functions, the slope is almost the same for both the simulated and measured results. High-pass transfer functions have the slope of attenuation of 38 dB per decade, band-pass functions have 19 dB per decade and in case of low-pass transfer functions it is 40 dB per decade. The ability to adjust the pole frequency and quality factor of the proposed filter has been discussed. The pole frequency can be changed without affecting the quality factor of the filter. While adjusting the quality factor the pole frequency of the filter slightly changes. When comparing the pole frequency, values obtained from the S-E filter are closer to the theoretical ones than values obtained from F-D structure. Values of the quality factors of the S-E filter are closer to the calculated ones. From the comparison of values of the quality factor it can be seen that values obtained from simulations are at lower values of the quality factor closer to the calculated values in both cases while changing g_{m3} and R_m.

Acknowledgement
Research described in the paper was supported by Czech Science Foundation project under No. 14-24186P, internal grant No. FEKT-S-14-2352 and by project OPVK CZ.1.07/2.2.00/28.0062 Joint activities of BUT and TUO while creating the content of accredited technical courses in ICT.
The described research was performed in laboratories supported by the National Sustainability Program under grant LO1401.

References:

[1] C. Toumazou, F. J. Lidgey, D. G. Haigh, Analog IC design: the current-mode approach, Institution of Electrical Engineers, London, 1996, 646 pages.

[2] J. Koton, N. Herencsar, K. Vrba, Single-Input Three-Output Current-Mode Filter Using Dual-Output Current Conveyors, In Proc.*Int. Conference on Electrical and Electronics Engineering* - ELECO 2009, Vol. 2, Turkey: EMO Yayinlari, 2009, pp. 263-266.

[3] H. P. Chen, P. L. Chu, Versatile universal electronically tunable current-mode filter using CCCIIs,*IEICE Electronics Express*, Vol. 6, No. 2, 2009, pp. 122-128.

[4] Ch. Chang, T. Huang, S. Tu, Ch. Hou, J. Horng, Universal Active Current Filter Using Single Second-Generation Current Controlled Conveyor, *RECENT ADVANCES IN SYSTEMS, COMMUNICATIONS & COMPUTERS, Selected Papers from the WSEAS Conferences in Hangzhou*, China, April 6-8, 2008, pp. 129-133.

[5] M. Sagbas, K. Fidaboylu, Electronically tunable current-mode second order universal filter using minimum elements,*Electronics Letters*, Vol.40, 2004, pp. 2-4.

[6] H. Chen, Current-mode dual-output ICCII-based tunable universal biquadratic filter with low-input and high-output impedances, *Int. J. Circ. Theor. Appl*., Vol. 42, Issue 4, Oct. 2012, pp. 376–393.

[7] H. Chen, Tunable versatile current-mode universal filter based on plus-type DVCCs, *AEU - International Journal of Electronics and Communications*, Vol. 66, Issue 4, 2012, pp. 332–339.

[8] J. Jerabek, R. Sotner, K. Vrba, Tunable universal filter with current follower and transconductance amplifiers and study of parasitic influences, *Journal of Electrical Engineering*, Vol. 62, No. 6, 2011, pp. 317-326.

[9] R. Sotner, J. Petrzela, J. Slezak, Current-Controlled Current-Mode Universal Biquad Employing Multi- Output Transconductors. *Radioengineering*, Vol. 18, No. 3, 2009, pp. 285-294.

[10] J. Jerabek, K. Vrba, Design of Fully Differential Filters with Basic Active Elements Working in the Current Mode. *Elektrorevue - Online Journal* (http://www.elektrorevue.cz), Vol. 2010, No. 87, pp. 1-5.

[11] N. A. Shah, M. Quadri, S. Z. Iqubal, Realization of CDTA based current-mode universal filter, *Indian J. pure & applied physics*, Vol. 46, 2008, pp. 283-285.

[12] D. Biolek, V. Biolkova, CDTA-C current-mode universal 2nd-order filter, *in proc. of the 5th WSEAS Int. Conf. on APPLIED INFORMATICS and COMMUNICATIONS*, Malta, September 15-17, 2005, pp. 411-414.

[13] R. S. Tomar, S. V. Singh, C. Chauhan, Fully Integrated Electronically Tunable Universal Biquad Filter Operating in Current-Mode, In Proc. the *international Conference Signal Processing and Integrated Networks* (SPIN), Noida, India,2014, pp. 549-554.

[14] R. S. Tomar, S. V. Singh, D. S. Chauhan, Cascadable Low Voltage Operated Current-Mode Universal Biquad Filter, *WSEAS TRANSACTIONS on SIGNAL PROCESSING*, Vol. 10, 2014, pp. 345-353.

[15] W.Jaikla, S. Siripongdee, P. Suwanjan, MISO current-mode biquad filter with independent control of pole frequency and quality factor,*Radioengineering*, Vol. 21, No. 3, 2012, pp. 886-891.

[16] S. V. Singh, S. Maheshwari, J. Mohan, D. S. Chauhan, Electronically tunable current-mode universal biquad filter based on the CCCCTA, In Proc. of *IEEE Int. Conf. on Advances in Recent Technologies in Comm. and Computing* (ARTCOM), 2009, pp. 424-429.

[17] A. Chaichana, M. Kumngern, W. Jaikla, Electronically Tunable Versatile Current-Mode MISO Universal Filter Including Minimum Component Count Circuits, *The 11th International Conference Electrical Engineering/Electronics, Computer, Telecommunications and Information Technology (ECTI-CON)*, 2014, 14-17 May, Nakhon Ratchasima, Thailand, pp. 1-4.

[18] D. Biolek, V. Biolkova, Z. Kolka, J. Bajer, Single-Input Multi-Output Resistorless Current-Mode Biquad, In proc. of *the European Conference on Circuit Theory and*

Design ECCTD 2009, Antalya, Turkey, 23-27 Aug. 2009, pp. 225 - 228.

[19] D. Biolek, V. Biolkova, Current-Input Current-Output 2nd-Order All-Pass Filter Employing Two ZC-CITAs, In proc. of *the 20th International Conference Radioelektronika (RADIOELEKTRONIKA) 2010*, Brno, Czech Republic, 19-21 Apr. 2010, pp. 1-4.

[20] L. Langhammer, J. Jerabek, Fully Differential Universal Current-Mode Frequency Filters Based on Signal-Flow Graphs Method, *International Journal of Advances in Telecommunications, Electrotechnics, Signals and Systems*, Vol. 3, No. 1, 2014, pp. 1-12.

[21] J. Jerabek, K. Vrba, Comparison of the Fully-Differential and Single-Ended Solutions of the Frequency Filter with Current Followers and Adjustable Current Amplifier, In Proc. *ICN2012 The Eleventh International Conference on Networks*, Reunion, France: IARIA, 2012, pp. 50-54.

[22] J. Jerabek, J. Koton, R. Sotner, K. Vrba, Adjustable band-pass filter with current active elements: two fully-differential and single-ended solutions, *Analog Integr. Circ. Sig. Process*., Vol. 74, 2013, pp.129–139.

[23] J. Koton, N. Herencsar, K. Vrba, I. Koudar, Fully differential current-mode filters using digitally adjustable current amplifier, *Elektrorevue - Online Journal* (http://www.elektrorevue.cz), No. 45, pp. 45-1–45-4.

[24] W. Tangsrirat, D. Prasertsom, Electronically tunable low-component-count current-mode biquadratic filter using dual-output current followers, *Electr. Eng.*Vol. 90, 2007, pp. 33–37.

[25] H. A. Alzaher, A CMOS Digitally Programmable Universal Current-Mode Filter, *IEEE Transactions on circuits and systems—II: Express briefs*, Vol. 55, No. 8, 2008, pp. 758-762.

[26] D. Prasertsom W. Tangsrirat, CMOS Digitally Controlled Current Follower and Its Application, In proc. of the *12th International Symposium on Integrated Circuits, ISIC '09*, Singapore, Republic of Singapore, 14-16 Dec. 2009, pp. 486 - 489.

[27] N. S. Nise, *Signal-Flow Graphs, The Control Handbook*, IEEE Press, 1996, 1566 pages.

[28] R. Sponar, K. Vrba, Measurements and Behavioral Modeling of Modern Conveyors, *International Journal of Computer Science and Network Security*, Vol. 3A, No. 6, 2006, pp. 57-63.

[29] J. Jerabek,R. Sotner, K. Vrba, Comparison of the SITO Current-Mode Universal Filters Using Multiple- Output Current Followers. In Proc. of *the 35th International Conference on Telecommunications and Signal Processing* (TSP 2012), pp. 406-410.

[30] D. Biolek, R. Senani, V. Biolkova, Z. Kolka, Active Elements for Analog Signal Processing: Classification, Review, and New Proposals. *Radioengineering*, Vol. 17, No. 4,2008, pp. 15-32.

[31] A. Gupta, R. Senani, D. R. Bhaskar, A. K. Singh, New OTRA-Based Generalized Impedance Simulator, *ISRN Electronics*, Vol. 5, 2013, pp. 1-10.

[32] Texas Instruments - OPA860 - Wide Bandwidth Operational Transconductance Amplifier (datasheet). Online, <http://www.ti.com/lit/ds/symlink/opa860.pdf>

[33] Texas Instruments - OPA861 - Wide Bandwidth Operational Transconductance Amplifier (datasheet). Online, <http://www.ti.com/lit/ds/symlink/opa861.pdf>